ALGEBRAIC TURBULENCE MODELS FOR UNSTRUCTURED MESHES[1]

Mgr. Vít Dolejší, Dr.,
Prof. RNDr. Miloslav Feistauer, DrSc.,
RNDr. Jiří Felcman, CSc.
Institute of Numerical Mathematics
Faculty of Mathematics and Physics
Charles University
Praha

Abstract

We deal with the numerical simulation of compressible turbulent flow. To discretize the system of the Navier–Stokes equations the operator splitting method is applied. To simulate the turbulence effect two algebraic turbulence models are implemented in our codes. To determine the turbulence viscosity the local structured mesh is constructed. At each time step, the values of physical quantities are interpolated from the global unstructured mesh to the local structured one, the turbulence model is executed on this mesh, and the resulting turbulence viscosity values are interpolated back to the global triangulation. Both method, Baldwin–Lomax model and Cebeci–Smidt model, were tested for the flow past cascade of profiles and the results are compared.

1 Introduction

The use of unstructured mesh techniques for computational fluid dynamics problems become more widespread in recent years, due to the flexibility they afford in discretizing arbitrarily complex geometries, and due to the possibility they offer in resolving highly localized flow phenomena through the use of adaptive meshing. During last years we have developed numerical schemes for the numerical simulation of viscous compressible (laminar) flow on unstructured meshes (see [2], [4]). Applying the strategy of the anisotropic mesh adaptation [1] we receive the solution in good correspondence with experimental measurements. But for the flow with high Reynolds number, we cannot neglect the turbulence effect, so that we employed an algebraic turbulence model which is easy to implement in our codes. The numerical scheme rests the same, only the viscous coefficient is replaced by the sum of the molecular and turbulent viscosities. The advantage of algebraic models is that no additional equations have to be solved, only the "correction" of viscous coefficient is performed. For computation of the turbulence viscosity we use similar approach as in [5].

2 Governing Equations

Let $\Omega \subset I\!R^2$ be a computational domain and $(0,T)$ a time interval. The system of the Navier – Stokes equations including an algebraic model of turbulence can be written in the conservative form

$$\frac{\partial \boldsymbol{w}}{\partial t} + \sum_{s=1}^{2} \frac{\partial \boldsymbol{f}_s(\boldsymbol{w})}{\partial x_s} = \sum_{s=1}^{2} \frac{\partial \boldsymbol{R}_s(\boldsymbol{w}, \nabla \boldsymbol{w})}{\partial x_s} \qquad \text{in } \Omega \times (0,T). \tag{1}$$

The viscous part of the stress tensor and the heat flux are given by

$$\begin{aligned} \boldsymbol{w} &= \boldsymbol{w}(x,t) = (w_1, w_2, w_3, w_4)^T = (\rho, \rho v_1, \rho v_2, e)^T, \ x \in \Omega, \ t \in (0,T), \\ \boldsymbol{f}_s(\boldsymbol{w}) &= (\rho v_s, \rho v_s v_1 + \delta_{s1} p, \rho v_s v_2 + \delta_{s2} p, (e+p) v_s)^T, \ s = 1, 2, \end{aligned} \tag{2}$$

[1]This work was supported under the grant No. 201/96/0313 of the Czech Grant Agency.

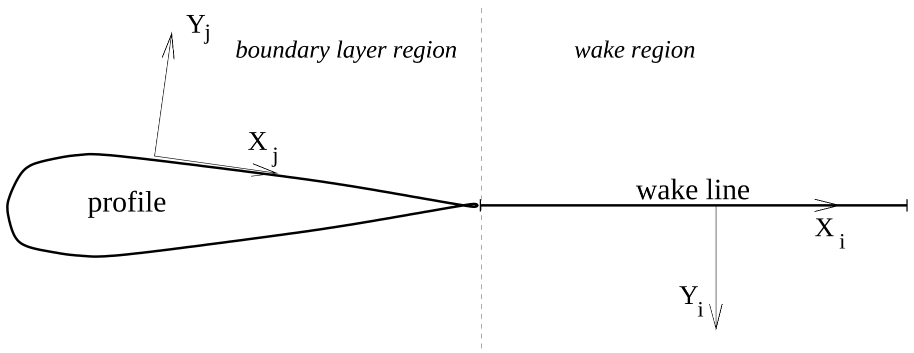

Figure 1: Local coordinate systems for algebraic turbulence model

$$
\begin{aligned}
R_s(\boldsymbol{w}, \nabla \boldsymbol{w}) &= (0, \tau_{s1}, \tau_{s2}, \tau_{s1}v_1 + \tau_{s2}v_2 - q_s)^T, \; s = 1,2, \\
\tau_{sl} &= (\mu + \mu_t)\left(\frac{\partial v_s}{\partial x_l} + \frac{\partial v_l}{\partial x_s} - \frac{2}{3}\delta_{sl} \operatorname{div} \boldsymbol{v}\right), \; s,l = 1,2, \\
q_s &= \frac{\gamma}{\gamma - 1}\left(\frac{\mu}{Pr} + \frac{\mu_t}{Pr_t}\right)\frac{\partial}{\partial x_s}\left[\frac{p}{\rho}\right], \; s = 1,2.
\end{aligned}
$$

The notation is standard: ρ – density, $\boldsymbol{v} = (v_1, v_2)$ – velocity vector, p – pressure, e – total energy, θ – absolute temperature, δ_{sl} – Kronecker delta, $\gamma > 1$ – Poisson adiabatic constant, μ – molecular viscosity, μ_t – turbulent viscosity, Pr – Prandtl number and Pr_t – turbulent Prandtl number. The molecular viscosity is given by the Sutherland law

$$
\mu = \mu_0 \left(\frac{\theta}{\theta_0}\right)^{1.5} \frac{\theta_0 + \tilde{\theta}}{\theta + \tilde{\theta}}, \tag{3}
$$

where $\theta_0 = p_{out}/(\rho_{int}(\gamma - 1))$ is the reference temperature, $\mu_0 = 6.6 \cdot 10^{-7}$, $Pr = 0.72$ and $Pr_t = 0.9$. The constant $\tilde{\theta}$ in (3) was set by Sutherland $\tilde{\theta} = 110$. As we use the nondimensional quantities we put $\tilde{\theta} = 110 \cdot \theta_0/300$. It rests to determinate the turbulent viscosity μ_t.

3 Algebraic Turbulence Models

The description of turbulence models can be found e.g. [7], [6]. First we must decide if the node, where we compute μ_t, belongs to the boundary layer or to the wake, i.e. we split the computational domain Ω onto two disjoint regions: *boundary layer region* and *wake region.* The splitting is viewed at Fig. 1. The boundary between these regions is perpendicular to the wake and the direction of the wake line is determined by the computation without turbulence model (see Sec.4.4). The boundary layer region lies from the separation line against the direction of the flow.

Then we introduce the set of local coordinate systems X_iY_i, $i \in I$, where I is a suitable index set, with the origin on the solid wall (profile) or in the middle of the wake (see Fig. 1). In the following we omit the index $_i$. The axis Y of each system is perpendicular to the solid wall (profile) or to the wake. By U, V we denote the $X-$, $Y-$ component of velocity in system XY, respectively.

The turbulent viscosity is computed using a two-layer approach,

$$
\mu_t = \begin{cases} \mu_{ti} & \text{if } Y \le Y_c \\ \mu_{to} & \text{if } Y > Y_c, \end{cases} \tag{4}
$$

where Y is the normal distance from the surface and Y_c is the least value of Y at which $\mu_{ti} = \mu_{to}$. The region where $Y \le Y_c$ we call *the inner layer* and the region where $Y > Y_c$ *the outer layer.* For the wake region the inner layer is not defined so that we have $\mu_t = \mu_{to}$.

3.1 Baldwin–Lomax Model

In the inner layer for Baldwin–Lomax model, we have

$$
\begin{aligned}
\mu_{ti} &= \rho K^2 Y^2 F_D^2 |\omega|, \\
F_D &= [1 - \exp(-Y^+/A^+)],
\end{aligned}
\tag{5}
$$

where ω is the vorticity

$$
\omega = \frac{\partial U}{\partial Y} - \frac{\partial V}{\partial X} \tag{6}
$$

and

$$
Y^+ = Y \frac{(\rho_w |\sigma_U|)^{1/2}}{\mu_w}. \tag{7}
$$

The subscript w denotes values taken at the origin of coordinate system XY, and σ_U is the local shear stress in the direction of the flow

$$
\sigma_U = \mu_w \frac{\partial U}{\partial Y}. \tag{8}
$$

The model constants are $K = 0.4$ and $A^+ = 26$.

In the outer layer

$$
\mu_{to} = \rho \alpha C_{cp} F_w F_{k_{BL}}, \tag{9}
$$

where

$$
\begin{aligned}
F_w &= \min(F_{w_1}, F_{w_2}), \\
F_{w_1} &= Y_{max} F_{max}, \\
F_{w_2} &= C_{wk} Y_{max} \frac{\Delta U^2}{F_{max}}.
\end{aligned}
\tag{10}
$$

The value F_{max} is the maximum of the function

$$
F = Y |\omega| F_D, \tag{11}
$$

over $(X, Y) \in \overline{\Omega},\ X = \text{const}$. In (11) Y_{max} is the value where $F(Y_{max}) = F_{max}$ and ΔU is the difference between maximum and minimum of the component velocity U over $(X, Y) \in \overline{\Omega},\ X = \text{const}$.

Additionally, the Klebanoff intermittency factor, $F_{k_{BL}}$, is given by

$$
F_{k_{BL}} = \left[1 + 5.5 \left(C_{KL} \frac{Y}{Y_{max}} \right)^6 \right]^{-1}, \tag{12}
$$

The model constants are $\alpha = 0.0168$, $C_{cp} = 1.6$, $C_{KL} = 0.3$ and $C_{wk} = 0.25$.

To summarize we can put $\mu_t = \min(\mu_{ti}, \mu_{to})$, where μ_{ti} and μ_{to} are given by (5) and (9) and $\mu_{ti} := \infty$ for the wake.

3.2 Cebeci–Smith Model

For the inner layer, we use the same relations as for the Baldwin–Lomax model, i.e. the relations (5) – (8) are the same and also the model constants K and A^+ have the same values.

In the outer layer we have

$$
\mu_{to} = \rho \alpha U_e \delta_i^* F_{k_{CS}}, \tag{13}
$$

with *the boundary layer displacement thickness*,

$$
\delta_i^* = \int_0^\delta \left(1 - \frac{U}{U_e} \right) dY, \tag{14}
$$

with U_e being the velocity at the boundary layer edge and δ the *boundary layer thickness* itself. In (13), the Clauser parameter α is taken to be a constant $\alpha = 0.0168$, and the Klebanoff intermittency function is derived as

$$F_{k_{CS}} = \left[1 + 5.5\left(\frac{Y}{\delta}\right)^6\right]^{-1}. \tag{15}$$

To summarize we can put $\mu_t = \min(\mu_{ti}, \mu_{to})$, where μ_{ti} and μ_{to} are given by (5) and (13) and $\mu_{ti} := \infty$ for the wake.

4 Implementation

4.1 Numerical Scheme

To solve the system of the Navier–Stokes equations, we use *the operator splitting method*, i.e. we split the system (1) into two subsystems: inviscid

$$\frac{\partial \boldsymbol{w}}{\partial t} + \sum_{s=1}^{2} \frac{\partial \boldsymbol{f}_s(\boldsymbol{w})}{\partial x_s} = 0 \qquad \text{in } \Omega \times (0,T). \tag{16}$$

and purely viscous

$$\frac{\partial \boldsymbol{w}}{\partial t} = \sum_{s=1}^{2} \frac{\partial \boldsymbol{R}_s(\boldsymbol{w}, \nabla \boldsymbol{w})}{\partial x_s} \qquad \text{in } \Omega \times (0,T). \tag{17}$$

and each of them we discretize separately. The inviscid system is discretized by the cell-centred *finite volume (FV) method* on a mesh $\mathcal{D}_h = \{D_i\}_{i\in J}$. Here the finite volumes D_i are triangles and $\mathcal{D}_h$ is a triangulation of the computational domain Ω. The *purely viscous system* is discretized by the conforming piecewise linear *finite elements (FE)* on a triangulation $\mathcal{T}_h$ of Ω, compatible with $\mathcal{D}_h$ in such sense that the set of all vertices P_i of the triangles $T \in \mathcal{T}_h$ consists of the barycentres of all $D_i \in \mathcal{D}_h$ and the vertices of $D_i \in \mathcal{D}_h$ lying on $\partial\Omega$. We call this mesh $\mathcal{T}_h$ *adjoint* to the grid $\mathcal{D}_h$. Using the above ideas, we discretize the complete system (1) via *operator inviscid-viscous splitting*. One time step $t_k \to t_{k+1}$ is divided into two *fractional steps*:

1. *Inviscid FV step on the mesh* $\mathcal{D}_h$: Assume that the values w_i^k, $i \in J$, approximating the solution on the finite volumes D_i at time t_k are known. Compute the values $w_i^{k+1/2}$, $i \in J$, from the FV formula

$$w_i^{k+1/2} = w_i^k - \frac{\tau_k}{|D_i|} \sum_{j\in S(i)} H(w_i^k, w_j^k, \boldsymbol{n}_{ij})\, \boldsymbol{n}_{ij}, \tag{18}$$

   where $S(i)$ denotes the set of neighbours triangles of D_i.

2. *Viscous FE step on the mesh* $\mathcal{T}_h$: Define the finite element function $w_h^{k+1/2}$ with values $w_h^{k+1/2}(P_i) = w_i^{k+1/2}$ at the vertices P_i, $i \in J$ of $\mathcal{T}_h$. At the vertices $P_i \in \partial\Omega_h$, the viscous Dirichlet boundary conditions and suitable extrapolation are used. Compute the finite element function w_h^{k+1} as the solution of the following problem:

   (a) w_h^{k+1} satisfies the viscous Dirichlet boundary conditions,

   (b)

$$(w_h^{k+1}, \varphi_h)_h = (w_h^{k+1/2}, \varphi_h)_h - \tau_k\, a_h(w_h^{k+1/2}, \varphi_h) \tag{19}$$

   for all test functions $\varphi_h = (\phi_1, ..., \phi_4)$ such that ϕ_j $(j = 1, ..., 4)$ is continuous in Ω, linear on each $T \in \mathcal{T}_h$ and vanishes on the part of $\partial\Omega$, where the j-th component w_j of the state vector w satisfies the Dirichlet boundary condition.

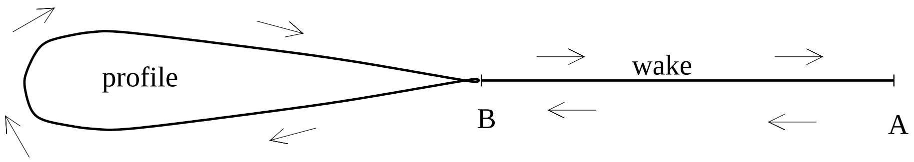

Figure 2: Basic line for the local triangulation

In (18), H is a suitable numerical flux approximated

$$H(w_i^k, w_j^k, \boldsymbol{n}_{ij}) \approx \int_{\Gamma_{ij}} \sum_{s=1}^{2} f_s(w(x, t_k))(\boldsymbol{n}_{ij})_s \, dS, \tag{20}$$

where Γ_{ij} denotes the common side between D_i and D_j and $(\boldsymbol{n}_{ij})_1, (\boldsymbol{n}_{ij})_2$ are the components of the unit outer normal $\boldsymbol{n}_{ij}$ on Γ_{ij} pointed out of D_i.

In (19), $(w, \varphi)_h$ and $a_h(w, \varphi)$ denote the approximation

$$\begin{aligned} (w, \varphi)_h &\approx \int_\Omega w \, \varphi \, dx, \\ a_h(w, \varphi) &\approx \int_\Omega \sum_{s=1}^{2} R_s(w, \nabla w) \, \partial\varphi / \partial x_s \, dx, \end{aligned} \tag{21}$$

obtained with the aid of numerical quadrature using the vertices of $T \in \mathcal{T}_h$ as integration points. For more detail see [3].

We perform the first FV step, then we compute the turbulent viscosity μ_t and we perform the FE step. The general procedure employed for implementing an algebraic turbulence model on an unstructured mesh consists of constructing local structured mesh about wall boundaries (see [5]). Each time the turbulence routine is called, the current flow variables are interpolated from the unstructured mesh onto the local structured turbulence mesh. The algebraic turbulence model is executed on this mesh and the resulting turbulence viscosity values are interpolated back to the unstructured mesh.

4.2 Construction of the Local Turbulence Mesh

We construct the local triangulation $\mathcal{L}_h$ in the following way. At first we define the basic line. It consists of two parts: profile, which is a closed curve, and the wake, which is a "two-side" abscissa (see Fig. 2). The profile curve is given by the geometry of the considered problem and the wake line is predetermined by solving the viscous flow (without any model of turbulence) over the entire configuration (see Sec. 4.4).

Now we can define the set of nodes of $\mathcal{L}_h$ which lie on the basic line. The nodes of the adjoint triangulation $\mathcal{T}_h$ lying on the profile we denote by $M_i,\ i = 0, \ldots, m$, where $M_0 = M_m = B$. For the wake part (between AB) we generate a new set of nodes $N_i,\ i = 0, \ldots, n$ in such a way that $N_i \in AB,\ i = 0, \ldots, n,\ N_0 = B,\ N_n = A$ and the distance between N_0 and N_1 denoted by $|N_0 N_1|$ is equal to $s_x = \min_{i=1,m} |M_{i-1} M_i|$. Then the distances of the abscissas $N_{i-1} N_i,\ i = 1, \ldots, n$ are given by

$$|N_{i-1} N_i| = |N_0 N_1| \cdot z_x^{i-1}, \quad i = 1, \ldots, n, \tag{22}$$

where $z_x \geq 1$ is a suitable real number.

Then we define the abscissas (which we will call the stations) $p_i,\ i = 0, \ldots, m$ and $q_i^1, q_i^2,\ i = 0, \ldots, n$ such that $M_i \in p_i,\ i = 0, \ldots, m$ and $N_i \in q_i^1, N_i \in q_i^2,\ i = 0, \ldots, n$ are the initial points. Moreover $p_i,\ i = 0, \ldots, m$ and $q_i^1, q_i^2,\ i = 0, \ldots, n$ are perpendicular to the basic line. Further, the stations $q_i^1,\ i = 0, \ldots, n$ and $q_i^2,\ i = 0, \ldots, n$ are oriented to the right and to the left with

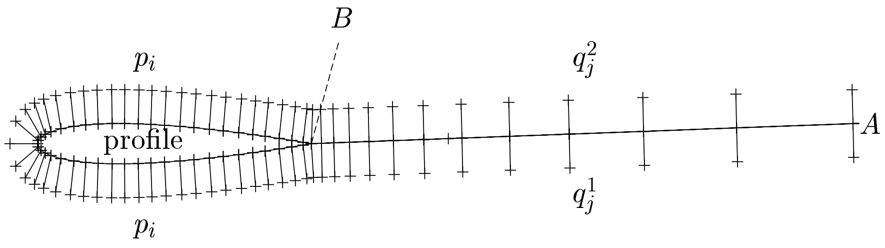

Figure 3: The stations $p_i,\ q_i^1,\ q_i^2$.

respect to the direction of the flow, respectively (see Fig. 3). The lengths of $p_i,\ i=0,\dots,m$ and $q_i^1, q_i^2,\ i=0,\dots,n$ are equal to

$$|p_i| = |q_j^1| = |q_j^2| = c_{part} r_{length}, \quad i=0,\dots,m,\ j=0,\dots,n, \tag{23}$$

where r_{length} is the diameter of profile (the characteristic length) and c_{part} is a positive constant (we use $c_{part}=0.1$). In the case of concave basic line, these stations have to be slightly perturbed so that no intersection of $p_i,\ i=0,\dots,m$ is presented.

For simplicity we put

$$\left\{ \begin{array}{lll} R_i = N_{n+1-i}, & r_i = q^1_{n+1-i}, & i=1,\dots,n, \\ R_{i+1+n} = M_i, & r_{i+1+n} = p_i, & i=0,\dots,m, \\ R_{i+1+m+n} = N_i, & r_{i+1+m+n}, = q_i^2, & i=1,\dots,n, \end{array} \right\} \tag{24}$$

and

$$k = 2n+m+1. \tag{25}$$

So that we have k nodes lying on the basic line. Some of them have the same coordinates.

Now we can construct the local triangular mesh. We put

$$s_y = \min_{T\in B} height(T), \quad B = \{T \in \mathcal{T}_h, T \text{ is a triangle adjacent to the profile}\}, \tag{26}$$

where $height(T)$ means the height of the triangle $T \in B$, the base side is the side adjacent to the profile.

We define the local grid as the set of nodes $\{X_{ij}\}_{i=1,\dots,k}^{j=1,\dots,l}$ by

$$\begin{array}{ll} X_{i1} = R_i, & i=1,\dots,k \\ X_{ij} \in r_i, & i=1,\dots,k, \quad j=2,\dots,l \\ |X_{ij}X_{i(j+1)}| = s_y \cdot z_y^{(j-1)}, & i=1,\dots,k, \quad j=2,\dots,l, \end{array} \tag{27}$$

where $z_y \ge 1$ is a suitable real number. The number l is given the maximal possible integer number such that

$$\sum_{j=1}^{l-1} |X_{ij}X_{i(j+1)}| \le c_{part} r_{length}, \tag{28}$$

where c_{part} is given by (23). Each element of this quadrilateral grid we divide onto two triangles and the local triangular mesh $\mathcal{L}_h$ arises (see Fig. 4).

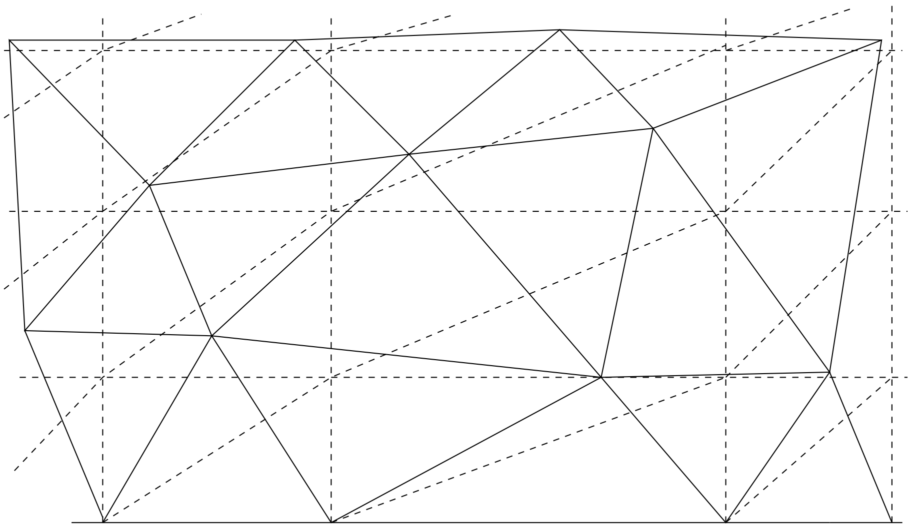

Figure 4: Local triangular mesh (the dashed line) and the global unstructured mesh (full line).

4.3 Interpolation Procedure

To execute the turbulence model, flow variables must be interpolated from the unstructured mesh onto the local turbulence mesh, and the resulting turbulence viscosity values must be interpolated back onto the unstructured mesh. The reconstruction is defined by the following way. Let $u = u(x, y),\ (x, y) \in \Omega$ be a function continuous piecewise linear for each $T \in T_h$. Let $X_{ij},\ i = 1, \ldots, k,\ j = 1, \ldots, l$ be the node of $\mathcal{L}_h$ with the coordinates $(x_{ij}, y_{ij}) \in \Omega$. Then the interpolated value of u in X_{ij} is given by

$$\tilde{u}(X_{ij}) = u(x_{ij}, y_{ij}), \qquad i = 1, \ldots, k,\ j = 1, \ldots, l. \tag{29}$$

So that for each X_{ij} we have to know only the index of triangle $T \in T_h$ for which $X_{ij} \in T$ and three interpolation coefficients which can be determined from the geometrical consideration. All these parameters are computed in advance and rest the same during all iterative process. The interpolation from the local mesh to the global unstructured mesh is performed in the same way, only in those nodes of $\mathcal{T}_h$, which are not covered by $\mathcal{L}_h$, we put in advance the turbulent viscosity equal to zero.

4.4 Setting of the Wake

We precise the setting the wake line for the generation of $\mathcal{L}_h$. The position of B is given from the geometry of the problem (the trailing edge, the point of the maximal curvature, etc.). To set the position of A we use the physical property that the vorticity changes the sign crossing the wake or the magnitude of velocity is minimal (see Fig. 5). The first position of A is determined form the viscous flow (without model of turbulence), we perform the computation including the algebraic turbulence model and after we determined the position of wake for each $q_i^1 \cap q_i^2,\ i = 0, \ldots, m$. Then the position of A can be corrected.

4.5 Implementation of the Algebraic Turbulence Models

In this subsection we would specify some special aspects of implementation of the algebraic models of turbulence. Some of them are common to both models and for other we specify the turbulence model.

- *Interpolation to the local turbulence mesh:* we use the interpolated technique described in Sec. 4.3. We interpolate the quantities ρ, v_1, v_2, e and also the derivations $\partial v_1/\partial x_1$,

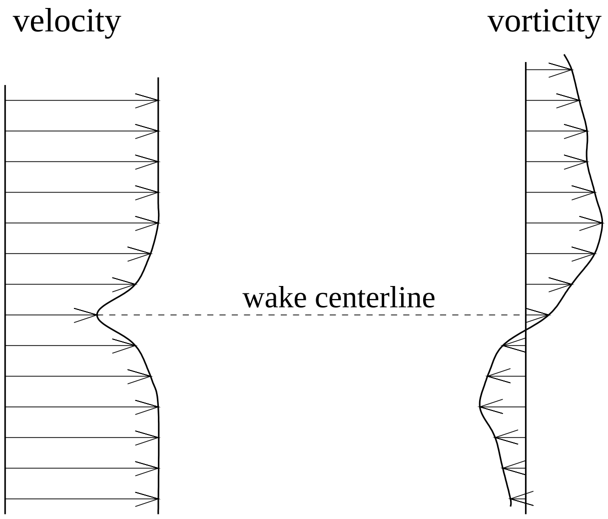

Figure 5: Determination of the position of the wake for algebraic turbulence model

$\partial v_1/\partial x_2$, $\partial v_2/\partial x_1$, $\partial v_2/\partial x_2$, which are computed in advance at the nodes of the adjoint triangulation $\mathcal{T}_h$ as the weighted average of derivatives on triangles with common node. As the weight the area of triangle is used. Then we can interpolate the values of $\partial v_1/\partial x_1$, $\partial v_1/\partial x_2$, $\partial v_2/\partial x_1$, $\partial v_2/\partial x_2$ to the local mesh $\mathcal{L}_h$ and the transformations to the local systems X_i, Y_i are performed (see Fig. 1). As the vorticity $\omega = \partial U/\partial Y - \partial V/\partial X$ is invariant with respect to the rotation we can put $\omega = \partial v_1/\partial x_2 - \partial v_2/\partial x_1$. Then we compute for each node of $\mathcal{L}_h$ the others quantities (absolute temperature, molecular viscosity, etc.) in its local coordinate system.

- *Inner Boundary layer:* We go successively over all stations adjacent to the profile. At first we determine the values of μ_w and σ_U for a given station. Then for all nodes of this given station the values F_D are determined and therefore the quantity μ_{ti}.

- *Outer Boundary Layer for Baldwin–Lomax:* We go successively over all stations beginning at the profile. For a given station we go over all its nodes and we compute quantities F_D and F, and we also find the extreme values y_{max}, F_{max} and ΔU for whole station. The minimal velocity is set to the zero (no-slip condition) so that ΔU is equal the maximal velocity U. At the end we go through all nodes of given station and we successively set the values F_w, $F_{k_{BL}}$ and μ_{to}.

- *Outer Boundary Layer for Cebeci–Smith:* At first we have to determine for each station the boundary layer thickness δ as the distance between wall and the points, where $U = 0.9 \cdot U_e$. The quantity U_e represents the velocity of the flow out of the boundary layer or wake. We define U_e as the maximal velocity on the station. Then we can easy compute the integral (14), where we integrate over the station from 0 to δ distance, and set δ_i^* and $F_{k_{CS}}$. Therefore we have μ_{to}.

- *Wake for Baldwin-Lomax:* Here we put automatically $\mu_{ti} = \infty$ and $F_D = 1$. At first we associate the opposite stations corresponding to the wake, i.e. the stations which have the common node at the wake centerline, $q_i = q_i^1 \cup q_i^2, \imath = 0, \ldots, n$. We go successively over all double stations $q_i = q_i^1 \cup q_i^2, \imath = 0, \ldots, n$. For each station we set *the local center wake point*, i.e. the node where the sign of vorticity is changed (Sec. 4.4). For ideal case this point is lying on the center wake line. In general case this point is very close to this line. Then we shift the coordinate system of the corresponding double station to the local center wake point Further we determine the values F for all nodes of the given double station and we also find the extreme values y_{max}, F_{max} and ΔU for whole double station.

At the end we go through all nodes of given double station and we successively set the values F_w, F_{kBL} and μ_{to}.

- *Wake for Cebeci-Smith:* Here we put automatically $\mu_{ti} = \infty$. The computation of μ_{to} is the same as for the outer boundary layer, where the integration goes (instead from profile) from the point laying on the wake centerline to the distance δ.

- To simulate transition from laminar to turbulent flows, Baldwin–Lomax proposed to set μ_t equal to zero everywhere in the wall-normal profile, for which the (tentatively) computed values μ_t is less then a pre-specified value

$$\mu_t \leq \mu_{infty} C_{\mathrm{MUTM}} \Longrightarrow \mu_t := 0, \qquad (30)$$

with a proposed values of $C_{\mathrm{MUTM}} = 14$. This technique we applied for Baldwin–Lomax as well as Cebeci–Smith models.

5 Numerical Results

Here we present the computation of the flow around SE1050 cascade of profiles. We use the following data: $\rho_{in} = 1$, $p_{out} = 3.01044889$, (therefore $\theta_0 = 0.8304440938$), $|\boldsymbol{v}_{in}| = 1$ and the angle of attack $\beta = 19^o 18'$. These boundary conditions yield to the outlet Mach number $M_{out} = 1.89$. Our results are compared with the experimental measurement, which was carried out at the Institute of Thermomechanic of Academy of Science of the Czech Republic (see [8]). The Fig. 6 shows the computational mesh, which represents one period of cascade of profiles, i.e. the periodic boundary conditions are considered. The triangulation was constructed by the anisotropic mesh adaptation generator [1]. The mesh alignment along shock waves, boundary layers and a wake was automatically performed. The results (the isolines of Mach number) of the "laminar computation" are presented at Fig. 7. The Baldwin–Lomax model and the Cebeci–Smidt model are presented at Fig. 8 and Fig. 9, respectively. Fig. 10 shows the comparison of the pressure distribution along the profile of all three computations with experimental results. We see the slight difference between two models of turbulence. From Fig. 10 we can have a sense that the computation without model of turbulence gives better results than the computation including turbulence models. But the experimental measurement is threedimensional and our computation only twodimensional so that this dimensional restriction can have higher influence than computation with/without model of turbulence.

The following table compares the drag and lift coefficients:

method	c_D	c_L
no turbulence	0.3449123	0.3272945
Baldwin–Lomax	0.3365613	0.3212661
Cebeci–Smidt	0.3361715	0.3208379

The coefficients are defined by

$$\begin{aligned} c_D &= \frac{1}{\frac{1}{2}\rho_\infty |u_\infty|^2} \int_\Gamma \left(\sum_{j=1}^{2} [\tau_{1j} n_j] - p_\infty n_1 \right) dx, \\ c_L &= \frac{1}{\frac{1}{2}\rho_\infty |u_\infty|^2} \int_\Gamma \left(\sum_{j=1}^{2} [\tau_{2j} n_j] - p_\infty n_2 \right) dx, \end{aligned} \qquad (31)$$

where Γ represents the boundary of the profile, (n_1, n_2) is the outer unit normal to the profile and $\tau_{ij},\ i,j = 1,2$ is given by (2).

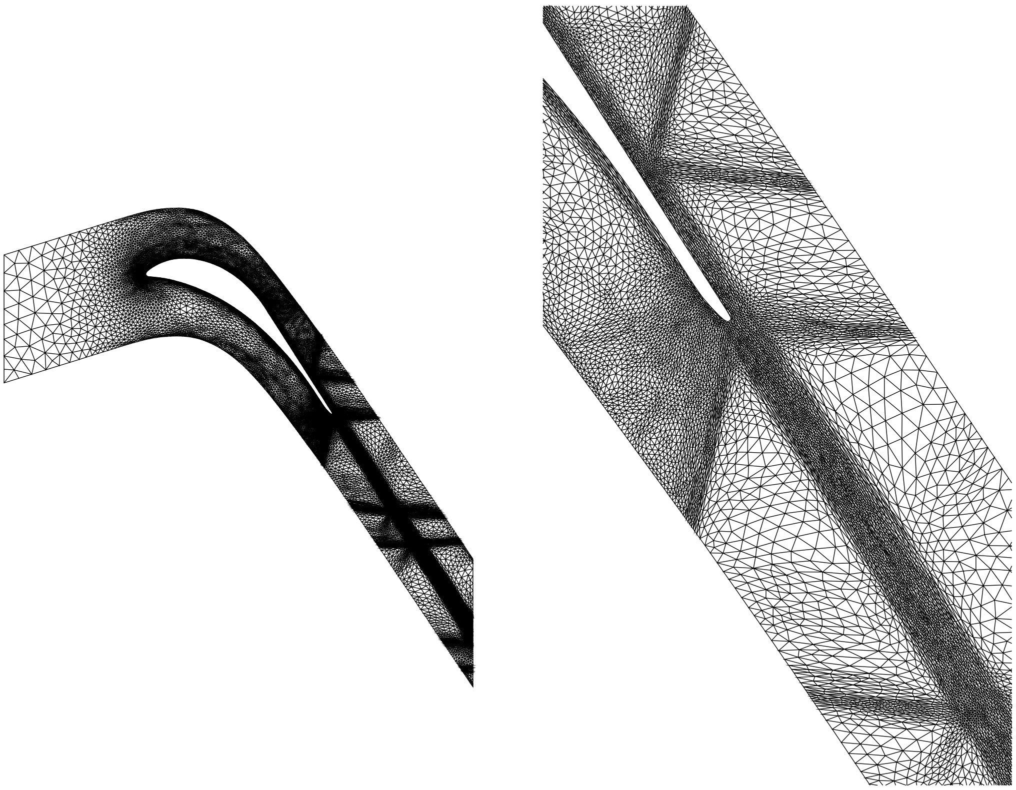

Figure 6: Triangulation of the computational domain and its detail

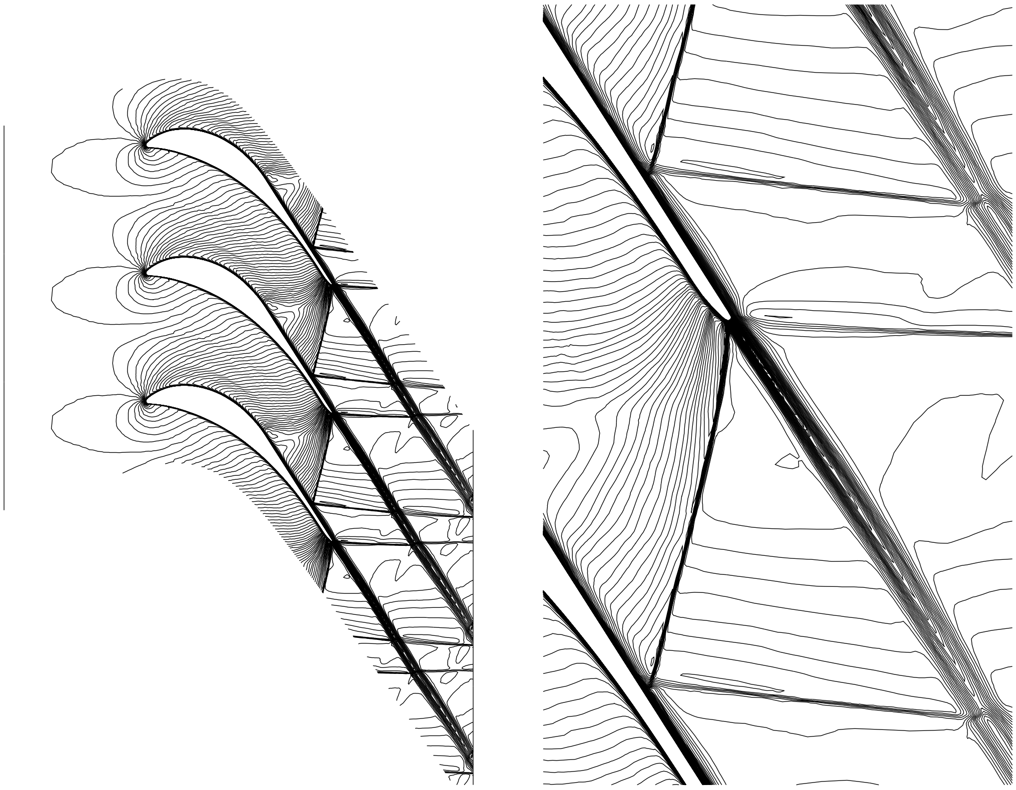

Figure 7: No turbulence model: Isolines of the Mach number and their detail

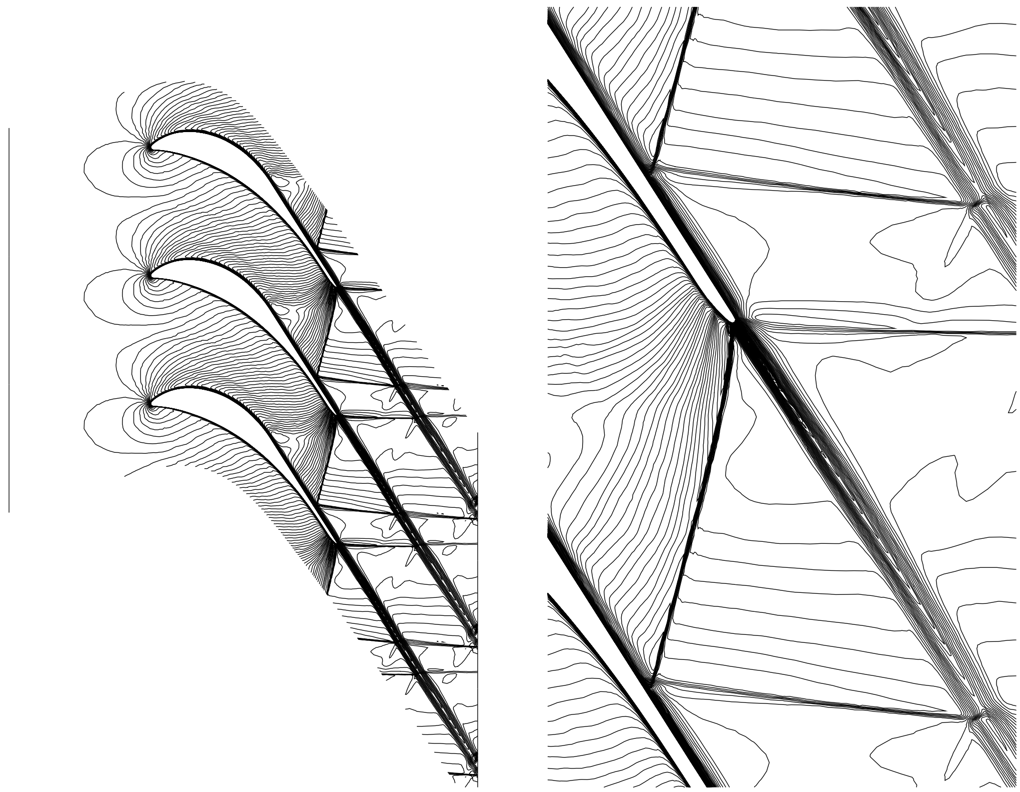

Figure 8: Baldwin–Lomax: Isolines of the Mach number and their detail

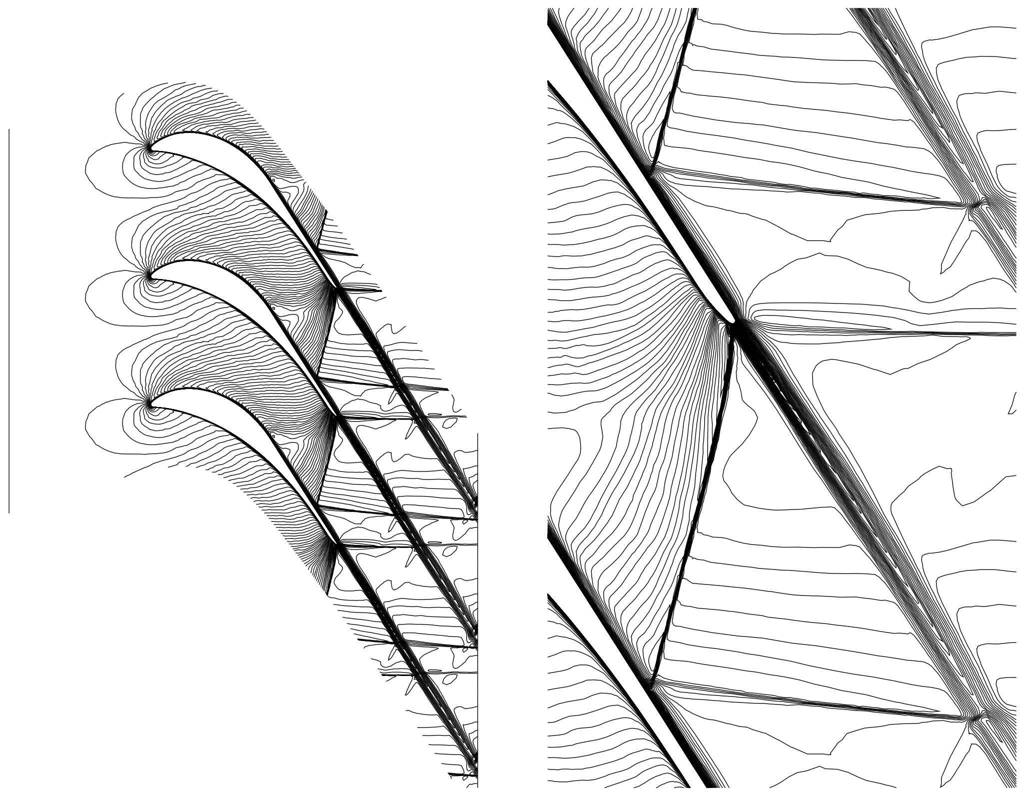

Figure 9: Cebeci–Smidt: Isolines of the Mach number and their detail

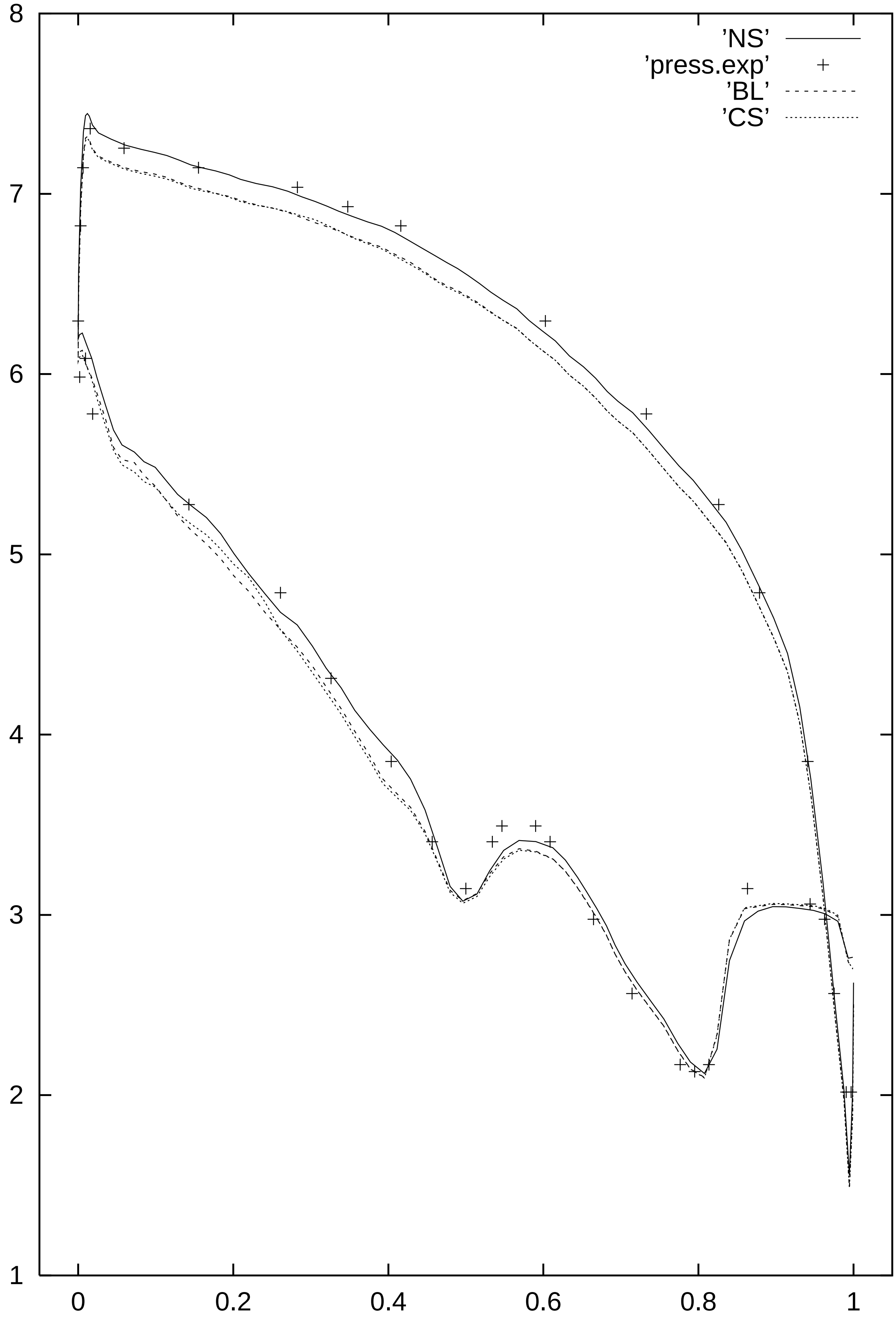

Figure 10: Distribution for the pressure along the profile. Comparison of the experimental measurement (+), no turbulence model (full line), Baldwin–Lomax model (dashed line) and Cebeci–Smith (pointed line).

References

[1] V. Dolejší. Anisotropic mesh adaptation for finite volume and finite element methods on triangular meshes. *Computing and Visualisation in Science*, 1998. to appear.

[2] V. Dolejší. Higher Order Finite Volume Methods for Compressible Flows. In K. Kozel and J. Příhoda, editors, *Dynamika tekutin'96*, pages 9–10. Ústav termomechaniky AV ČR, Praha, 1996. ISBN 80-85918-23-4.

[3] M. Feistauer, J. Felcman, and V. Dolejší. Numerical Simulation of Compresssible Viscous Flow through Cascades of Profiles. *ZAMM*, 76:297–300, 1996.

[4] J. Felcman and V. Dolejší. Adaptive Methods in Internal and External Flow Computations. In M. P. Bendsøe M. Brøns and M. P. Sørensen, editors, *Progress in Industrial Mathematics at ECMI 96*, pages 424–431. B. G. Teubner, Stuttgart, 1997. ISBN 3-519-02607-4.

[5] Dimitri J. Mavriplis. Algebraic turbulence modelling for unstructured and adaptive meshes. *AIAA Journal*, 29(12):2086–2093, 1991.

[6] Notes on Numerical Fluids Dynamics: 58. ECARP-European Computational Aerodynamics Research Project. In Werner Hasse, Eric Chaput, Eberhard Elsholz, Michael A. Leschziner, and Udo R. Müller, editors, *Validation of CFD and Assessment of Turbulence Models*, 1997.

[7] J. Příhoda. Algebraické modely turbulence a jejich použití při řešení středovaných Navier–Stokesových rovnic. Technical report, Ústav termomehcaniky ČSAV, 1990. Z-1153/90.

[8] M. Šťastný and P. Šafařík. Experimental Analysis Data on the Transonic Flow Past a Plane Turbine Cascade. *ASME Paper 90-GT-313, New York*, 1990.